

Defects responsible for charge carrier removal and correlation with deep level introduction in irradiated $\beta\text{-Ga}_2\text{O}_3$

A. Y. Polyakov,¹ N. B. Smirnov,¹ I. V. Shchemerov,¹ E. B. Yakimov,^{1,2} S. J. Pearson,^{3,a)} Chaker Fares,⁴ Jiancheng Yang,⁴ Fan Ren,⁴ Jihyun Kim,⁵ P. B. Lagov,^{1,6} V. S. Stolbunov,⁷ and A. Kochkova¹

¹National University of Science and Technology MISIS, 4 Leninsky Ave., Moscow 194017, Russia

²Institute of Microelectronics Technology and High Purity Materials, Russian Academy of Science,

6 Academician Ossipyan Str., Chernogolovka, Moscow Region 142432, Russia

³Department of Materials Science and Engineering, University of Florida, Gainesville, Florida 32611, USA

⁴Department of Chemical Engineering, University of Florida, Gainesville, Florida 32611, USA

⁵Department of Chemical and Biological Engineering, Korea University, 145, Anam-ro, Seongbuk-gu, Seoul, South Korea

⁶Laboratory of Radiation Technologies, A.N. Frumkin Institute of Physical Chemistry and Electrochemistry Russian Academy of Sciences (IPSE RAS), 31 Leninsky Ave., Moscow 119071, Russia

⁷Institute of Theoretical and Experimental Physics Russian Academy of Science (ITEP RAS), 25 B. Cheremushkinskaya St., Moscow 117218, Russia

(Received 19 July 2018; accepted 14 August 2018; published online 30 August 2018)

Carrier removal rates and electron and hole trap densities in $\beta\text{-Ga}_2\text{O}_3$ films grown by hydride vapor phase epitaxy (HVPE) and irradiated with 18 MeV α -particles and 20 MeV protons were measured and compared to the results of modeling. The electron removal rates for proton and α -radiation were found to be close to the theoretical production rates of vacancies, whereas the concentrations of major electron and hole traps were much lower, suggesting that the main process responsible for carrier removal is the formation of neutral complexes between vacancies and shallow donors. There is a concurrent decrease in the diffusion length of nonequilibrium charge carriers after irradiation, which correlates with the increase in density of the main electron traps E2* at $E_c - (0.75\text{--}0.78)$ eV, E3 at $E_c - (0.95\text{--}1.05)$ eV, and E4 at $E_c - 1.2$ eV. The introduction rates of these traps are similar for the 18 MeV α -particles and 20 MeV protons and are much lower than the carrier removal rates. Published by AIP Publishing. <https://doi.org/10.1063/1.5049130>

$\beta\text{-Ga}_2\text{O}_3$ is attracting interest because of its large bandgap of 4.8 eV, high electric breakdown field of 8 MV/cm, and high saturation electron velocity of 2×10^7 cm/s, which make it promising for high-power devices and solar-blind photodetectors.^{1–9} Advances in growth technology have resulted in good crystalline and electrical quality bulk and epitaxial n-type material prepared by various techniques, while progress in device fabrication and processing has made it possible to demonstrate high-power rectifiers,¹⁰ field effect transistors (FETs) based on $\beta\text{-Ga}_2\text{O}_3$ thin films^{10–12} or nanobelts,^{13,14} and sensitive solar-blind photodetectors.¹⁵

Theoretical studies have clarified the role of oxygen vacancies as deep donors, gallium vacancies and their complexes with hydrogen as deep compensating acceptors, and Si, Ge, and Sn as shallow donors.^{16–21} Theory also points to the absence of impurities suitable as shallow acceptor dopants and the role of polaronic states of self-trapped holes (STHs) that result in low hole mobility even when nonequilibrium holes are created by illumination.^{17,22} Studies using the Hall effect,^{23,24} deep level transient spectroscopy (DLTS),^{23–28} deep level optical spectroscopy (DLOS),^{23,27} admittance spectroscopy (AS),^{29,30} light capacitance voltage (LCV) profiling, photocapacitance spectroscopy (PC),^{23,28–30} photoluminescence (PL) and micro-cathodoluminescence (MCL) spectroscopy,^{31,32} localized vibrational mode (LVM)

spectroscopy,³³ positron annihilation (PA),³⁴ and electron beam induced current (EBIC)^{28,35} have established the positions of major electron traps in the upper half and deep acceptors in the lower half of the bandgap and compensation by gallium vacancy acceptors or their complexes with shallow donors in as-grown or irradiated films and crystals and the energy level positions of transition metal impurities such as Fe.^{23,26} EBIC and DLTS measurements with optical excitation (ODLTS) demonstrate that nonequilibrium holes are mobile in $\beta\text{-Ga}_2\text{O}_3$ at moderate temperatures, with an activation energy of transition from polaronic STH states to valence band holes being lower than predicted.^{17,22,28,30,35} A better understanding of the defects in $\beta\text{-Ga}_2\text{O}_3$ is necessary to assess the role this material will play relative to the established wide-bandgap materials SiC and GaN in further evolution of high-power electronics and optoelectronics. In this paper, we report measurements of electrical and recombination properties and deep trap spectra in $\beta\text{-Ga}_2\text{O}_3$ irradiated with protons and α -particles to clarify the role of deep traps in compensation of conductivity and in recombination processes.

The samples were grown by hydride vapor phase epitaxy (HVPE) on bulk substrates prepared by the edge-defined film-fed growth method. The growth plane was (100), with Si doping in the HVPE films [donor concentration $(2\text{--}4) \times 10^{16}$ cm⁻³]. The substrates were heavily doped with Sn (donor concentration of 3×10^{18} cm⁻³). The film

^{a)}Author to whom correspondence should be addressed: spear@mse.ufl.edu

thickness after chemomechanical polishing was $10\text{ }\mu\text{m}$, while the substrates were $650\text{-}\mu\text{m}$ -thick. The properties were studied before and after irradiation at 25°C with 18 MeV α -particles with a fluence of 10^{13} cm^{-2} and with 20 MeV protons with fluences of 5×10^{13} and 10^{14} cm^{-2} . Characterization included capacitance-voltage (C-V) profiling and LCV profiling with excitation from high-power (optical power: 250 mW) light emitting diodes (LEDs) with peak photon energies ranging from 1.35 eV to 3.4 eV or with UV LEDs emitting at a 250.4 nm wavelength (photon energy: 4.9 eV ; optical power: $300\text{ }\mu\text{W}$). Deep electron trap spectra were obtained from DLTS in the temperature range of $77\text{--}400\text{ K}$ using a cryostat or in the $290\text{ K}\text{--}470\text{ K}$ range using a hot plate. Hole trap spectra were obtained by ODLTS³⁶ with above-bandgap (4.8 eV) or below-bandgap (3.4 eV) LEDs. Diffusion lengths (L_d) of nonequilibrium charge carriers were calculated from the dependence of EBIC collection efficiency on the probing beam accelerating voltage of the scanning electron microscope (SEM).²⁸ All measurements were performed for samples with semi-transparent Ni Schottky contacts on the front and Ti/Au back Ohmic contact to the n^+ -substrate.^{10,28,29,36}

The damage profiles were obtained from the Stopping-and-Range-of-Ions-in-Matter (SRIM) code,^{37,38} which calculates the screened Coulombic collision rate between an incoming ion and the atoms in the target. An ion traversing the Ga_2O_3 undergoes collisions with the target atoms. The total energy loss per unit distance is determined by electronic stopping and nuclear stopping. In the former, ion energy is lost by excitation and ionization of atoms, dissipating as heat, and not creating atomic displacements. Nuclear stopping occurs through elastic collisions of ions with nuclei or atoms, with part of the kinetic energy of the incoming ion transferred to displace nuclei, creating deep-level compensating defects.

Figure 1 shows room temperature C-V profiles before and after irradiation with 18 MeV α -particles or 20 MeV protons (two fluences). Also shown are the starting profile and the profile after 10 MeV proton irradiation (fluence of 10^{14} cm^{-2}). The latter samples were studied previously.²⁸ For all three types of irradiation, the decrease in the net shallow donor concentration was significant, some 10^{16} cm^{-3} .

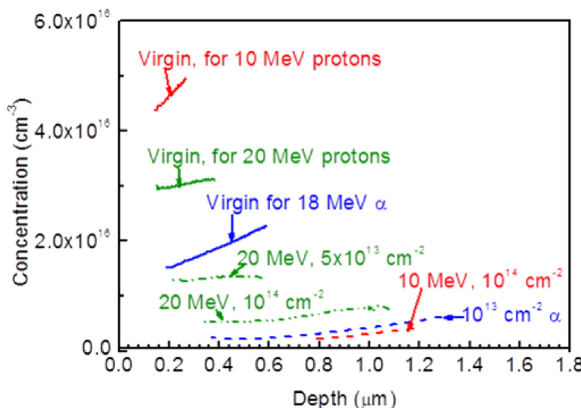


FIG. 1. C-V concentration profiles measured in Ga_2O_3 before irradiation and after irradiation with 10^{13} cm^{-2} 18 MeV α -particles, 10^{14} cm^{-2} 10 MeV protons, and 5×10^{13} and 10^{14} cm^{-2} 20 MeV protons.

The carrier removal was approximately linear with fluence in the case of 20 MeV protons, and the removal rates were 400 cm^{-1} for 10 MeV protons, $250\text{--}340\text{ cm}^{-1}$ for 20 MeV protons, and 1300 cm^{-1} for 18 MeV α -particles. To put these results into a more physical context, we calculated the densities of vacancies produced by 10^{14} cm^{-2} protons of two energies and by 10^{13} cm^{-2} fluence of 18 MeV α -particles using SRIM modeling. The results are presented in Fig. 2. The ranges of respective particles in $\beta\text{-Ga}_2\text{O}_3$ were estimated as $100\text{ }\mu\text{m}$ (18 MeV α -particles), $360\text{ }\mu\text{m}$ (10 MeV protons), and $1000\text{ }\mu\text{m}$ (20 MeV protons), with the vacancy concentrations in the region we are probing being in the range of $0.5\text{--}3 \times 10^{16}\text{ cm}^{-3}$ for 10 and 20 MeV protons and $\sim 3 \times 10^{16}\text{ cm}^{-3}$ for α -particles. Thus, the number of primary radiation defects, gallium vacancies, predicted by modeling is in reasonable agreement with the observed decreases in net shallow donor density. It is then important to identify the traps responsible for this donor compensation.

Figure 3(a) shows DLTS spectra after irradiation with α -particles for temperatures from $77\text{--}400\text{ K}$ in the cryostat (solid line) and from $290\text{--}470\text{ K}$ on the hot plate (dashed line). The starting spectra were similar for all samples before irradiation with α -particles or protons, although the absolute concentrations of traps slightly differed from sample to sample. The spectra showed a minor peak near 230 K corresponding to electron traps E1 with level $E_c - 0.6\text{ eV}$ [electron capture cross section $\sigma_n = (4\text{--}6) \times 10^{-15}\text{ cm}^2$], as well as peaks E2* [$E_c - (0.75\text{--}0.78)\text{ eV}$ and $\sigma_n = (1\text{--}3) \times 10^{-14}\text{ cm}^2$], E3 [$E_c - (0.95\text{--}1.05)\text{ eV}$ and $\sigma_n = (3.5\text{--}29) \times 10^{-14}\text{ cm}^2$], and E4 [$E_c - 1.2\text{ eV}$ and $\sigma_n = (4\text{--}15) \times 10^{-14}\text{ cm}^2$]. These are well documented electron traps and the notation follows that proposed previously.^{23,25,26,28}

After irradiation, new centers emerged at $E_c - 0.28\text{ eV}$ ($\sigma_n = 6 \times 10^{-18}\text{ cm}^2$) and, for α -particle irradiation, E5 ($E_c - 1.35\text{ eV}$ and $\sigma_n = 3 \times 10^{-12}\text{ cm}^2$) [Fig. 3(a)]. The spectrum in Fig. 3(a) is the DLTS signal $\Delta C/C$ multiplied by $2 N_d$ and by the DLTS spectrometer correlator function F^{-1} so the signal in the peaks corresponds to the trap concentration without the λ -correction³⁴ (ΔC is the capacitance difference at times corresponding to the chosen time windows, and C is the steady-state capacitance). Alpha-particle irradiation increased the concentration of all traps, but to a different

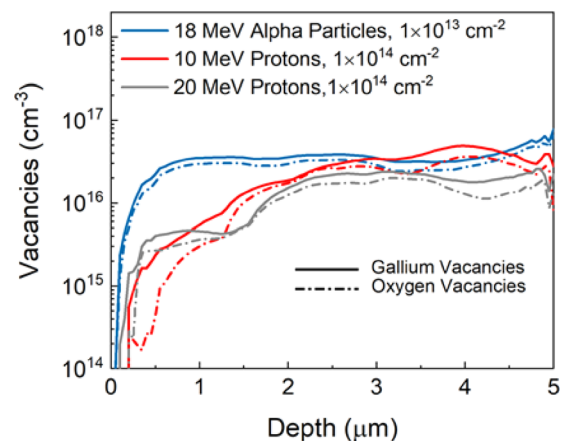


FIG. 2. SRIM modeling of Ga_v and O_v distributions in proton or alpha particle irradiated Ga_2O_3 .

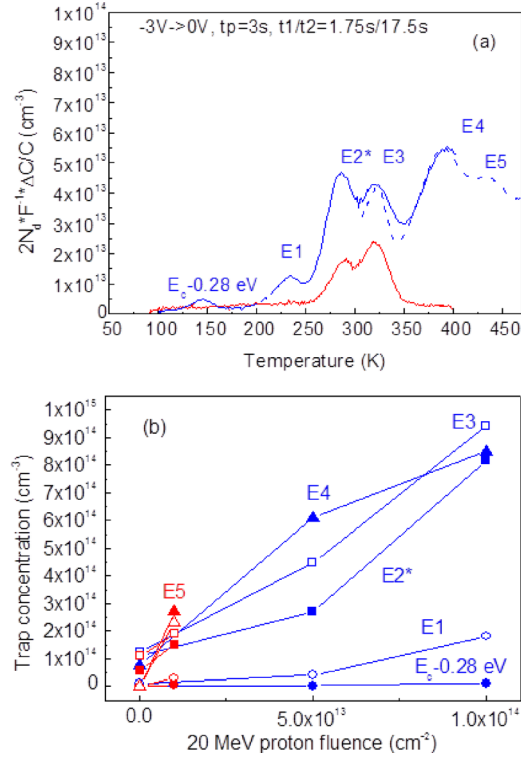


FIG. 3. (a) DLTS spectra of β -Ga₂O₃ before (red line) and after irradiation with 10^{13} cm^{-2} 18 MeV α -particles (blue line for measurements to 400 K; dashed blue line for the hot-stage measurement); bias -3 V, forward bias pulse 0 V (for 3 s), and time windows 1.75 s/17.5 s; (b) deep trap concentrations as a function of fluence, calculated with taking into account the λ -correction for the sample irradiated with α -particles (red lines and symbols) or with 20 MeV protons (blue lines and symbols).

extent. (The results for proton irradiation were similar; the spectra are not shown to save space.) Figure 3(b) shows the variation with dose of all detected electron traps for α -irradiation when the λ -correction is done. The figure also shows data for samples irradiated with 20 MeV protons—in that case, no E5 electron traps were detected. The main change comes from the E2* traps whose introduction rates are $\sim 8 \text{ cm}^{-1}$ for both types of irradiation and E3 and E4 traps with introduction rates $\sim 20 \text{ cm}^{-1}$ for α -particles and 8 cm^{-1} for 20 MeV protons. The introduction rates are more than an order of magnitude lower than the carrier removal rates so that, even if all these traps were acceptors, they could not account for the donor decrease after irradiation.

In DLTS measurements on the n-type material with Schottky diodes, it is difficult to effectively recharge electron traps with levels much deeper than the Schottky barrier height (about 1.2 eV in our case) and to recharge hole traps in the lower half of the bandgap by electrical pulsing.^{29,32} Also, it is difficult to probe states deeper than about 1.4–1.5 eV from respective band edges.²⁹ Here, states in the lower half of the bandgap were probed by PC and LCV measurements with monochromatic light excitation^{29,30} and by ODLTS. For un-irradiated samples, these methods did not reveal the presence of measurable concentrations of deep states in the lower half of the gap. After irradiation, we could detect features in LCV and PC spectra with optical thresholds near 1.35 eV, 2.1–2.3 eV, and 3.1 eV. Figure 4 shows room temperature LCV spectra for samples irradiated with 18 MeV α -particles (fluence of 10^{13} cm^{-2}) and 20 MeV

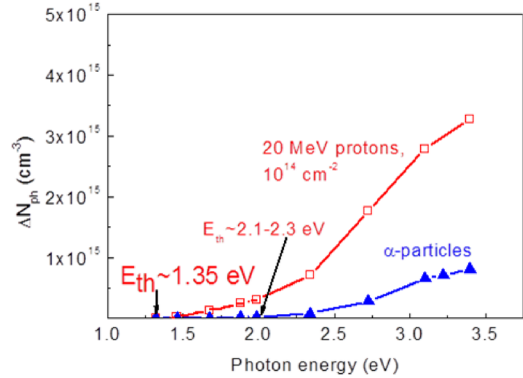


FIG. 4. The spectral dependence of the LCV concentration under illumination (ΔN_{ph}) with various photon energies for 20 MeV proton (red line and symbols) and 18 MeV α -particle (blue line and symbols) irradiation (the dark concentrations are subtracted).

protons (fluence 10^{14} cm^{-2}). For all three features in PC and LCV spectra, the photocapacitance changes after irradiation were persistent. However, the photocapacitance changes induced by photons with energies below 2.3 eV could not be quenched by application of high forward bias, indicating that the centers have a high barrier for capture of electrons.^{29,30} Similar traps with a strong lattice coupling have been observed in DLOS/PC spectra of β -Ga₂O₃.^{25,27} For higher photon energies, part of the persistent photocapacitance ($\sim 2/3$ of the total at photon energy 3.4 eV) could be quenched by application of forward bias. Such centers first emerged for photon energies near 3.1 eV. These deep centers in the lower half of the bandgap keep their nonequilibrium holes until they are thermally excited, since there are no electrons to recombine with holes on deep centers in the space charge region. Once electrons are provided by the application of the forward bias, the nonequilibrium hole charge is eliminated.^{29,30,40} Obviously, the latter centers are different from the centers with optical threshold near 2.3 eV in that they do not possess a high barrier for capture of electrons.

ODLTS spectra of irradiated samples showed a prominent signal from hole traps with activation energy near 1.4 eV for excitations with 3.4 eV photons and 4.8 eV photons. Figure 5 presents the spectrum for the α -irradiated sample for the 3.4 eV photon excitation (for the 4.8 eV excitation, a similar peak was observed, but the amplitude was about 5 times

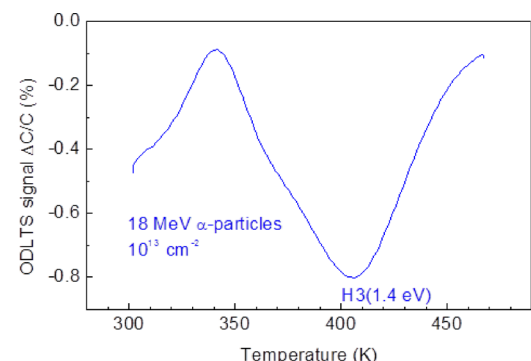


FIG. 5. ODLTS spectra measured with 3.4 eV LED excitation (5-s-long pulse) for the samples irradiated with 18 MeV α -particles; bias -1 V; time windows 1.25 s/12.5 s.

lower, most likely because the 4.8 eV UV LED power was about 1000 times lower than the 3.4 eV LED power and not sufficient to saturate the centers in question). We tentatively associate these traps observed in ODLTS with defects in the LCV spectra quenchable with forward bias application, although the question, of course, arises how the $E_v + 1.4$ eV traps can be excited by photons with an energy of 3.1 eV. The energy level of the $E_v + 1.4$ eV states determined from ODLTS is not far from the level near $E_v + 1.3$ eV ascribed to V_{Ga} acceptors.²⁴ The absolute concentrations of the centers in the lower half of the bandgap can be determined from LCV, provided that, for all photon energies, the photocapacitance signal saturates and that only one type of optical transitions is predominant.

In our case of n-type material, the traps with optical thresholds near 2.1–2.3 eV and 3.1 eV in PC and LCV spectra should be completely filled with electrons in the dark, so that saturation in their PC and LCV signals should correspond to the total concentration of traps unless the optical cross section for the transition from the valence band to the trap level partly emptied by light is high.⁴¹ Photocapacitance transient measurements confirm that for traps with optical thresholds of 2.1–2.3 eV and 3.1 eV, the PC signal is saturated and the optical cross section for transitions from the valence band to these centers is low. Thus, the LCV spectra measurements yield the full trap concentrations. For the 1.35 eV traps, the situation is more complicated because these will be filled only in the λ -region of the space charge region.³⁹ These traps are within reach of the standard DLTS measurements and thus have been already counted in DLTS, although it is not yet established which of the electron traps in DLTS correspond to the feature in PC/LCV. Figure 4 presents the LCV spectra of the α -particle and 20 MeV irradiated samples. The results indicate that the aggregate concentration of traps with optical thresholds of 2.1–2.3 eV and 3.1 eV is $3.5 \times 10^{15} \text{ cm}^{-3}$ for protons and $8 \times 10^{14} \text{ cm}^{-3}$ for α -particles, with $\sim 2/3$ of the signal coming from the quenchable hole traps. For the control samples, the concentration of the hole traps in the lower half of the bandgap as measured by LCV and photocapacitance was negligible.

Prior to irradiation, the diffusion length L_d was 600 nm. After irradiation with 20 MeV protons at a fluence of $5 \times 10^{13} \text{ cm}^{-2}$, L_d decreased to 330 nm and to 160 nm for a fluence of 10^{14} cm^{-2} . The diffusion length decreased with increasing density of major electron traps, the most abundant of which are the E2*, E3, and E4 traps. The dependence of $1/L_d^2 = N_t \sigma v_{th}/D$ (where σ is the capture cross section, v_{th} the thermal velocity, and D the diffusion coefficient of non-equilibrium carriers³⁵) on N_t was approximately linear, as shown in Fig. 6 for the E3 centers.

Our measurements suggest that the electron removal rate upon irradiation of $\beta\text{-Ga}_2\text{O}_3$ with protons and α -particles is close to the introduction rate of acceptor Ga_v determined by SRIM modeling. However, LCV spectra, photocapacitance spectra, and ODLTS measurements all show the concentrations of the Ga_v to be much lower than required to account for the observed carrier removal rates and this also goes for other prominent deep defects in the lower half of the bandgap, centers with optical threshold near 2.1–2.3 eV. The most dominant deep electron traps detected in irradiated

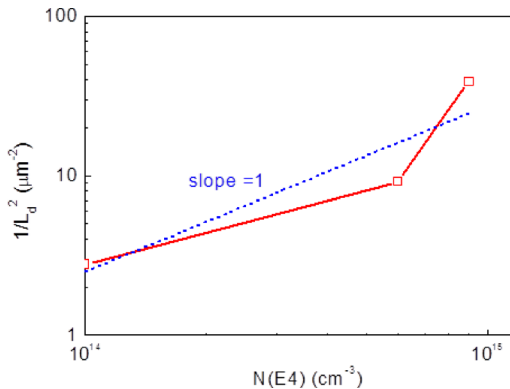


FIG. 6. $1/L_d^2$ as a function of concentration of E3 electron traps in 20 MeV protons irradiated samples.

samples in the upper half of the bandgap are the E2*, E3, and E4 traps^{23,25,26,28} with levels from 0.75–1.2 eV from the conduction band edge. The introduction rates of these traps are similar for the 18 MeV α -particles and 20 MeV protons and are much lower than the carrier removal rates. The major part of carrier removal comes from the primary radiation defects forming neutral complexes with shallow donors. The nature of radiation defects that form deep centers in the bandgap is not clear at the moment. The $E_v + 1.4$ eV acceptors could be related to not only the Ga_v acceptors that have not formed complexes with shallow donors but also the Ga_{v^-} acceptor complexes with hydrogen.^{19,33} The levels of electron traps E3 and E4 are close to the two deep oxygen vacancy V_O donors predicted by theory,¹⁸ and these could be associated with the lifetime degradation in irradiated $\beta\text{-Ga}_2\text{O}_3$.

The work at NUST MISiS was supported in part by the Ministry of Education and Science of the Russian Federation in the framework of Increase Competitiveness Program of NUST (MISiS, K2-2014-055). The work at UF was supported by Department of Defense, Defense Threat Reduction Agency, HDTRA1-17-1-011, monitored by Jacob Calkins. The research at Korea University was supported by the New and Renewable Energy Core Technology Program of the Korea Institute of Energy Technology Evaluation and Planning (KETEP) grant from the Ministry of Trade, Industry and Energy, Republic of Korea (Nos. 20173010012970 and 20172010104830). Proton irradiation was performed on injector-linear accelerator I-2 “Kamiks” at the Center of Collective Use at the Institute of Theoretical and Experimental Physics in Moscow.

¹See, for example, M. Higashiwaki and G. H. Jessen, *Appl. Phys. Lett.* **112**, 060401 (2018); J. Y. Tsao, S. Chowdhury, M. A. Hollis, D. Jena, N. M. Johnson, K. A. Jones, R. J. Kaplar, S. Rajan, C. G. Van de Walle, E. Bellotti, C. L. Chua, R. Collazo, M. E. Coltrin, J. A. Cooper, K. R. Evans, S. Graham, T. A. Grotjohn, E. R. Heller, M. Higashiwaki, M. S. Islam, P. W. Juodawlkis, M. A. Khan, A. D. Koehler, J. H. Leach, U. K. Mishra, R. J. Nemanich, R. C. N. Pilawa-Podgurski, J. B. Shealy, Z. Sitar, M. J. Tadjer, A. F. Witulski, M. Wraback, and J. A. Simmons, *Adv. Electron. Mater.* **4**, 1600501 (2018); M. A. Mastro, A. Kuramata, J. Calkins, J. Kim, F. Ren, and S. J. Pearton, *ECS J. Solid State Sci. Technol.* **6**, P356 (2017); S. J. Pearton, J. Yang, P. H. Cary, F. Ren, J. Kim, M. J. Tadjer, and M. A. Mastro, *Appl. Phys. Rev.* **5**, 011301 (2018).

- ²S. Krishnamoorthy, Z. Xia, C. Joishi, Y. Zhang, J. McGlone, J. Johnson, M. Brenner, A. R. Arehart, J. Hwang, S. Lodha, and S. Rajan, *Appl. Phys. Lett.* **111**, 023502 (2017).
- ³S. Rafique, L. Han, A. T. Neal, S. Mou, M. J. Tadjer, R. H. French, and H. Zhao, *Appl. Phys. Lett.* **109**, 132103 (2016).
- ⁴M. J. Tadjer, N. A. Mahadik, J. A. Freitas, E. R. Glaser, A. D. Koehler, L. E. Luna, B. N. Feigelson, K. D. Hobart, F. J. Kub, and A. Kuramata, *Proc. SPIE* **10532**, 1053212 (2018).
- ⁵C. Joishi, S. Rafique, Z. Xia, L. Han, S. Krishnamoorthy, Y. Zhang, L. Lodha, H. Zhao, and S. Rajan, *Appl. Phys. Express* **11**, 03110 (2018).
- ⁶M. J. Tadjer, N. A. Mahadik, V. D. Wheeler, E. R. Glaser, L. Ruppalt, A. D. Koehler, K. D. Hobart, C. R. Eddy, and F. J. Kub, *ECS J. Solid State Sci. Technol.* **5**, P468 (2016).
- ⁷A. J. Green, K. D. Chabak, M. Baldini, N. Moser, R. Gilbert, R. C. Fitch, G. Wagner, Z. Galazka, J. McCandless, A. Crespo, K. Leedy, and G. H. Jessen, *IEEE Electron Device Lett.* **38**, 790 (2017).
- ⁸K. Zeng, J. S. Wallace, C. Heimburger, K. Sasaki, A. Kuramata, T. Masui, J. A. Gardella, and U. Singisetti, *IEEE Electron Device Lett.* **38**, 513 (2017).
- ⁹H. Zhou, K. Maize, G. Qiu, A. Shakouri, and P. D. Ye, *Appl. Phys. Lett.* **111**, 092102 (2017).
- ¹⁰K. Konishi, K. Goto, H. Murakami, Y. Kumagai, A. Kuramata, S. Yamakoshi, and M. Higashiwaki, *Appl. Phys. Lett.* **110**, 103506 (2017).
- ¹¹M. H. Wong, K. Sasaki, A. Kuramata, S. Yamakoshi, and M. Higashiwaki, *IEEE Electron Device Lett.* **37**, 212 (2016).
- ¹²J. F. McGlone, Z. Xia, Y. Zhang, C. Joishi, S. Lodh, S. Rajan, S. A. Ringel, and A. R. Arehart, *IEEE Electron Device Lett.* **39**, 1042 (2018).
- ¹³J. Kim, M. A. Mastro, M. J. Tadjer, and J. Kim, *ACS Appl. Mater. Interfaces* **9**, 21322 (2017).
- ¹⁴J. Kim, S. Oh, M. A. Mastro, and J. Kim, *Phys. Chem. Chem. Phys.* **18**, 15760 (2016).
- ¹⁵A. M. Armstrong, M. H. Crawford, A. Jayawardena, A. Ahyi, and S. Dhar, *J. Appl. Phys.* **119**, 103102 (2016).
- ¹⁶J. B. Varley, J. R. Weber, A. Janotti, and C. G. Van de Walle, *Appl. Phys. Lett.* **97**, 142106 (2010).
- ¹⁷J. B. Varley, A. Janotti, C. Franchini, and C. G. Van de Walle, *Phys. Rev. B* **85**, 081109 (2012).
- ¹⁸L. Dong, R. Jia, B. Xin, B. Peng, and Y. Zhang, *Sci. Rep.* **7**, 40160 (2017).
- ¹⁹S. Lany, *APL Mater.* **6**, 046103 (2018).
- ²⁰P. Deák, Q. D. Ho, F. Seemann, B. Aradi, M. Lorke, and T. Frauenheim, *Phys. Rev. B* **95**, 075208 (2017).
- ²¹W. R. L. Lambrecht, D. Skachkov, A. Ratnaparkhe, H. J. von Bardeleben, U. Gerstmann, Q. D. Ho, and D. Peter, *Proc. SPIE* **10533**, 1053304 (2018).
- ²²A. Kyrtos, M. Matsubara, and E. Bellotti, *Appl. Phys. Lett.* **112**, 032108 (2018).
- ²³K. Irmscher, Z. Galazka, M. Pietsch, R. Uecker, and R. Fornari, *J. Appl. Phys.* **110**, 063720 (2011).
- ²⁴E. Chikoidze, A. Fellous, A. Perez-Tomas, G. Sauthier, T. Tchelidze, C. Ton-That, T. T. Huynh, M. Phillips, S. Russell, M. Jennings, B. Berini, F. Jomard, and Y. Dumont, *Mater. Today Phys.* **3**, 118 (2017).
- ²⁵Z. Zhang, E. Farzana, A. R. Arehart, and S. A. Ringel, *Appl. Phys. Lett.* **108**, 052105 (2016).
- ²⁶M. E. Ingebrigtsen, J. B. Varley, A. Y. Kuznetsov, B. G. Svensson, G. Alfieri, A. Mihaila, U. Badstüber, and L. Vines, *Appl. Phys. Lett.* **112**, 042104 (2018).
- ²⁷E. Farzana, E. Ahmadi, J. S. Speck, A. R. Arehart, and S. A. Ringel, *J. Appl. Phys.* **123**, 161410 (2018).
- ²⁸A. Y. Polyakov, N. B. Smirnov, I. V. Shchemerov, E. B. Yakimov, J. Yang, F. Ren, G. Yang, J. Kim, A. Kuramata, and S. J. Pearton, *Appl. Phys. Lett.* **112**, 032107 (2018).
- ²⁹A. Y. Polyakov, N. B. Smirnov, I. V. Shchemerov, D. Gogova, S. A. Tarelkin, and S. J. Pearton, *J. Appl. Phys.* **123**, 115702 (2018).
- ³⁰A. Y. Polyakov, N. B. Smirnov, I. V. Shchemerov, S. J. Pearton, F. Ren, A. V. Chernykh, P. B. Lagov, and T. V. Kulevoy, "Hole traps persistent photocapacitance proton irradiated β -Ga₂O₃ films doped with Si," *APL Mater.* (to be published).
- ³¹T. Onuma, S. Fujioka, T. Yamaguchi, M. Higashiwaki, K. Sasaki, T. Masui, and T. Honda, *Appl. Phys. Lett.* **103**, 041910 (2013).
- ³²H. Gao, S. Muralidharan, N. Pronin, M. R. Karim, S. M. White, T. Asel, G. Foster, S. Krishnamoorthy, S. Rajan, L. R. Cao, M. Higashiwaki, H. von Wenckstern, M. Grundmann, H. Zhao, D. C. Look, and L. J. Brillson, *Appl. Phys. Lett.* **112**, 242102 (2018).
- ³³P. Weiser, M. Stavola, W. B. Fowler, Y. Qin, and S. Pearton, *Appl. Phys. Lett.* **112**, 232104 (2018).
- ³⁴B. E. Kananen, L. E. Halliburton, K. T. Stevens, G. K. Foundos, K. B. Chang, and N. C. Giles, *Appl. Phys. Lett.* **110**, 202104 (2017); E. Korhonen, F. Tuomisto, D. Gogova, G. Wagner, M. Baldini, Z. Galazka, R. Schewski, and M. Albrecht, *Appl. Phys. Lett.* **106**, 242103 (2015).
- ³⁵E. B. Yakimov, A. Y. Polyakov, N. B. Smirnov, I. V. Shchemerov, J. Yang, F. Ren, G. Yang, J. Kim, and S. J. Pearton, *J. Appl. Phys.* **123**, 185704 (2018).
- ³⁶A. Y. Polyakov, N. B. Smirnov, I.-H. Lee, and S. J. Pearton, *J. Vac. Sci. Technol. B* **33**, 061203 (2015).
- ³⁷See, <http://www.srim.org/> for "Tutorial and Software Download."
- ³⁸J. F. Ziegler, M. D. Ziegler, and J. P. Biersack, *Nucl. Instrum. Methods Phys. Res. B* **268**, 1818 (2010).
- ³⁹A. R. Peaker, V. P. Markevich, and J. Coutinho, *J. Appl. Phys.* **123**, 161559 (2018).
- ⁴⁰A. Y. Polyakov and I.-H. Lee, *Mater. Sci. Eng. R* **94**, 1 (2015).
- ⁴¹D. K. Schroeder, *Semiconductor Material and Device Characterization* (John Wiley and Sons, New York, 1990).